metals

MDPI

Article

Quasi-Particle Approach to the Autowave Physics of Metal Plasticity

Lev B. Zuev * and Svetlana A. Barannikova

Institute of Strength Physics and Materials Science, Siberian Branch of Russian Academy of Sciences, 634055 Tomsk, Russia; bsa@ispms.tsc.ru

* Correspondence: lbz@ispms.tsc.ru; Tel.: +7-3822-491-360

Received: 28 September 2020; Accepted: 28 October 2020; Published: 29 October 2020

Abstract: This paper is the first attempt to use the quasi-particle representations in plasticity physics. The de Broglie equation is applied to the analysis of autowave processes of localized plastic flow in various metals. The possibilities and perspectives of such approach are discussed. It is found that the localization of plastic deformation can be conveniently addressed by invoking a hypothetical quasi-particle conjugated with the autowave process of flow localization. The mass of the quasi-particle and the area of its localization have been defined. The probable properties of the quasi-particle have been estimated. Taking the quasi-particle approach, the characteristics of the plastic flow localization process are considered herein.

Keywords: metals; plasticity; autowave; crystal lattice; phonons; localization; defect; dislocation; quasi-particle; dispersion; failure

1. Introduction

The autowave model of plastic deformation [1–4] admits its further natural development by the method widely used in quantum mechanics and condensed state physics. The case in point is the introduction of the quasiparticle exhibiting wave properties—that is, application of corpuscular-wave dualism [5]. The current state of such approach was proved and illustrated in [5].

Few attempts of application of quantum-mechanical representations are known in plasticity physics. They were focused, for example, on direct quantum-mechanical treatment of specific details of plastic flow mechanisms unexplained by traditional approaches. Thus, Bell [6] paid attention to possible quantization of elastic modules of materials, and Steverding [7] introduced the representation about quantization of elastic waves accompanying a destruction process. Later on, this problem in expanded interpretation was considered by Maugin [8] with application to solitons in elastic media. Gilman [9] and then Oku and Galligan [10] tried to use the tunnel effect to explain the dislocation breaking from obstacles at low temperatures when the thermal activation ceased to operate and estimated the probability of tunneling under these conditions. Petukhov and Pokrovskii [11] presented the well-founded and exact analysis of this phenomenon for dislocations moving in the Peierls potential relief. Recently, these problems have been repeatedly addressed in [12].

The other group of studies was apparently initiated by Morozov, Polak, and Fridman in their crucial work [13]. These authors analyzed the kinetics of growth of a fragile crack in a deforming medium and postulated the existence of a quasiparticle which they associated with the end of the growing fragile crack and called crackon. This idea was further used and developed to study mechanisms of strain-induced microdefects. Thus, Zhurkov [14] introduced the concept of elementary crystal excitation—dilaton—representing a negative density fluctuation. Olemskoi and Katsnelson [15] discussed the occurrence of the shear or destruction nuclei they called frustron.

These works were the first attempts to introduce the quantum representations into plasticity physics. They were crucial, because the existing plastic flow models in actual crystals with defects were completely based on principles of classical mechanics. At the same time, the crystal lattice theory is, generally speaking, quantum-mechanical in character. Such different approaches, obviously, make it difficult to construct a complete and physically well-founded plastic flow pattern.

The idea of the existence of the quasi-particle corresponding to the localized plastic flow autowave arises naturally against this background. Some aspects of this promising problem are studied in the present work. The approach developed here supplements the autowave mechanics of plasticity [1] and in our opinion, can be fruitful for an explanation of the main features of the plastic flow phenomenon.

The present study initiates the use of a quasi-particle model for the explanation of the localized plastic flow development in solids. A similar step matches the main directions in physics of solids [5].

2. Materials and Methods

The studies of localized plastic flow were performed for nineteen metals from the 3rd, 4th, 5th, and 6th periods of the Periodic Table of Elements (see the Table 1). The autowave characteristics of the localized plastic strain required for an analysis were obtained from visual pattern of their localized plasticity recorded by the speckle-photographic method (SPM) of analysis of deformation fields during elongation of flat samples described in detail in [1–4]. SPM has a field of vision of about 100 mm and resolution of about 1 μm comparable to that of optical microscopy. The method was realized using an Automatic Laser Measuring Complex (ALMEC), which enables one to reconstruct the displacement vector fields $\boldsymbol{r}(x, y)$ for the deforming flat sample and calculate all the plastic distortion tensor components—i.e.,

$$\beta_{ij} = \nabla \boldsymbol{r}(x, y) = \begin{pmatrix} \varepsilon_{xx} & \varepsilon_{xy} \\ \varepsilon_{yx} & \varepsilon_{yy} \end{pmatrix} + \omega_z,$$

where $\begin{pmatrix} \varepsilon_{xx} & \varepsilon_{xy} \\ \varepsilon_{yx} & \varepsilon_{yy} \end{pmatrix}$ is the plastic deformation tensor for plane specimen and ω_z is the rotation about the axis z. The plastic distortion tensor components are: longitudinal extension $\varepsilon_{xx} = \partial u/\partial x$, lateral contraction $\varepsilon_{yy} = \partial v/\partial y$, shear $\varepsilon_{xy} = \varepsilon_{yx} = 1/2(\partial v/\partial x + \partial u/\partial y)$, and rotation $\omega_z = 1/2(\partial v/\partial x - \partial u/\partial y)$. Here, $u = r\cos\phi$ and $v = r\sin\phi$ are, respectively, the longitudinal and the transverse components of the displacement vector r; ϕ is the angle the vector r makes with the sample extension axis, x. A computer program was written for creating data files $\varepsilon_{xx}(x, y)$, $\varepsilon_{yy}(x, y)$, $\varepsilon_{xy}(x, y)$ and $\omega_z(x, y)$. The results of calculations can be presented as components of the plastic distortion tensor distributed over the sample (see example in Figure 1).

Values of the parameters the wavelengths λ and the velocities V_{aw} were evaluated from the $X - t$ diagrams (X is the coordinate of the localized strain center in the laboratory system of coordinates and t is time), as described in [1–4] (see example in Figure 2), and the interplanar distance χ and the transverse ultrasonic wave rate in crystal V_t values were borrowed from the handbooks.

Table 1. Effective mass values (amu), calculated by Equation (1).

Mass	**Metals**										
$m_{ef}^{(emp)}$	Cu	Zn	Al	Zr	Ti	V	Nb	α-Fe	ɣ-Fe	Ni	Co
	1.8	1.1	0.5	2.0	1.1	1.4	2.3	1.8	1.8	1.9	1.3
$m_{ef}^{(emp)}$	Sn	Mg	Cd	In	Pb	Ta	Mo	Hf	-	-	-
	1.3	4.0	4.2	1.6	1.3	0.6	0.3	4.0	-	-	-

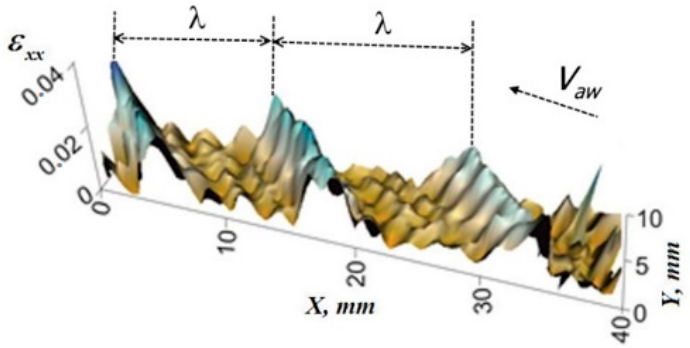

Figure 1. Spatial distribution of local elongations ε_{xx} over the test sample Al.

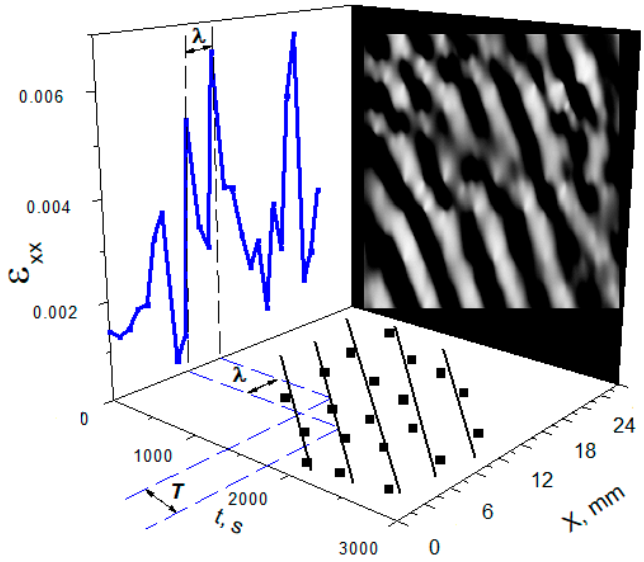

Figure 2. Localized plastic flow pattern: distribution of local elongations ε_{xx} observed for the sample midline; pattern observed for different times (dark and light bands correspond to active and passive material volumes, respectively); illustration of the method $X-t$ diagrams for measuring λ and T values.

3. Results

The results presented below and their interpretations are based on the experimental data obtained previously in the study of the autowave character of plastic flow development in materials of various kinds [1–4].

3.1. On the Possibility of Introduction of the Quasi-Particle

3.1.1. Mass Associated with the Localized Plasticity Autowave

The first well-known attempt of direct application of quantum-mechanical models for interpretation of localized plastic flow autowaves was undertaken by Billingsley [16]. He applied the de Broglie equation $m = h/\lambda V$, written for the mass, to the characteristics of the autowaves described in our works [17–19] and demonstrated that the calculated value correlates with the atomic mass of the investigated metal. In the above equation, h is the Planck constant and λ and V are the autowave wavelength and velocity, respectively.

This idea was further developed by us in [20,21], including an increase in the number of investigated materials and a more correct interpretation of the autowave characteristics of the deformation process. In [16], we wrote the de Broglie equation for the mass in the form

$$m_{ef}^{(emp)} = \frac{h}{\lambda V_{aw}} \tag{1}$$

where the wavelengths λ and the velocities V_{aw} of autowaves observed at the stages of linear work hardening of metals investigated by the present time we took from our investigations of the development of localized plasticity in nineteen metals. As follows from Table 1, the empirical effective masses calculated from Equation (1) lie within comparatively narrow limits $0.3 \le m_{ef}^{(emp)} \le 4.2$ amu (1 amu = 1.66×10^{-27} kg is the atomic mass unit).

The average effective mass calculated in this way was $\left\langle m_{ef}^{(emp)} \right\rangle = 1.7 \pm 0.3 \approx 2$ amu. The comparatively small variation of this value demonstrates that the masses calculated from Equation (1) are not occasional in character and are determined by the development of the localized plastic flow.

3.1.2. Nature of the Effective Mass

To elucidate the physical meaning of m_{ef}, we took into account that separate regions of a deforming material are involved in the process of plastic flow in a particular, serial order, one by one, during propagation of the phase localized plasticity autowave. Hence, the plastic deformation carriers–dislocations move with acceleration. In this case, the parameter m_{ef} can be interpreted as the attached mass caused by accelerated motion of dislocations in a viscous medium [22]. Such a medium in the case of plastic deformation can be the phonon and electronic gases of a metal crystal the viscosity of which was studied by Al'shits and Indenbom [23]. The dislocation motion dynamics during plastic flow is controlled by the viscous drag force (per unit length) $F_{vis} \sim BV_{disl}$ determined by the viscosity B of the phonon and electronic gases in a crystal [23]. This is correct, if $V_{disl} = const$, but when $V_{disl} \neq const$, the inertial term F_{in} proportional to the dislocation acceleration $\dot{V}_{disl} \neq 0$ is added to the force F_{vis} [22]. In this case,

$$F_\Sigma = F_{vis} + F_{in} \sim BV_{disl} + \frac{B}{\nu} \cdot \dot{V}_{disl} \sim B\left(V_{disl} + \frac{\dot{V}_{disl}}{\nu}\right) \tag{2}$$

In metals, the contributions of the phonon and electronic gases to the viscous drag coefficient of dislocations are additive—that is, $B = B_{ph} + B_e$ [23]. In this case, from Equation (2), it follows that

$$F_\Sigma \sim (B_{ph}V_{disl} + B_eV_{disl} + \frac{B_{ph}}{\nu}\dot{V}_{disl} + \frac{B_e}{\nu}\dot{V}_{disl}). \tag{3}$$

If ν is the frequency of deformation acts, the parameter B/ν can be interpreted as the attached mass per unit dislocation length. This coincides with the result obtained by Eshelby [24] according to which the dislocation motion is described by the same equation, as the motion of the Newton particle. Thus, the third and fourth terms in the right-hand side of Equation (3) are the attached mass—that is,

$$F_{in} \sim \frac{B_{ph} + B_e}{\nu}\dot{V}_{disl} \sim \left(\frac{B_{ph}}{\nu}\dot{V}_{disl} + \frac{B_e}{\nu}\dot{V}_{disl}\right). \tag{4}$$

The factors by the acceleration $\dot{V}_{disl}$ are the attached mass including, obviously, the contributions of the phonon, $m_{ph} \sim \left(B_{ph}/\nu\right)$, and electron gases, $m_e \sim (B_e/\nu)$, respectively. The phonon contribution depends weakly on the metal nature, because at $T > T_D$, where T_D is Debye's temperature [25], the metal properties are almost independent of the special features of its phonon spectrum. Thus, for example, the lattice (phonon) heat capacity at these temperatures is independent

of the material and temperature [25]. Based on the foregoing, we can set $F_{in}^{(ph)} \sim \left(B_{ph}/\nu\right)\dot{V}_{disl} \approx const$ and $m_{ph} \sim \left(B_{ph}/\nu\right) \approx const$. The contribution of electronic gas drag differs from the one described. According to [23], $B_e \approx B_0 + \kappa n$, where n is the electronic gas density (the number of conduction electrons per unit cell), and B_0 and κ are constants. Then, Equation (4) can be written in the form

$$F_{in}^{(e)} \sim \frac{B_e}{\nu} \cdot \dot{V}_{disl} \sim \frac{B_0 + \kappa n}{\nu} \cdot \dot{V}_{disl}. \quad (5)$$

In this case, the effective mass is $(B_0 + \kappa n)\nu^{-1} \sim n$, which is confirmed by the experimental data presented in [20] and shown in Figure 3. In this figure, by analogy with [20], the dimensionless mass $s = m_{ef}^{(emp)}/A$ is used instead of $m_{ef}^{(emp)}$, where A is the atomic mass of the corresponding element. From Figure 3, it is evident that the proportionality $s \sim n$ is satisfied for two periods of the Periodic Table of Elements. This result emphasizes a relationship of the macroscopic characteristics λ and V_{aw} of localized plastic deformation with the parameters of the electronic structure of a metal. The existence of the above-considered relationship of the kinetics of moving dislocations with the properties of the electronic gas is indirectly confirmed, for example, by the data presented in [26–28]. In these works, the authors have related the electric potential on the surface of a deforming metal sample with the entrainment of conduction electrons by moving dislocations during jump-like plastic deformation.

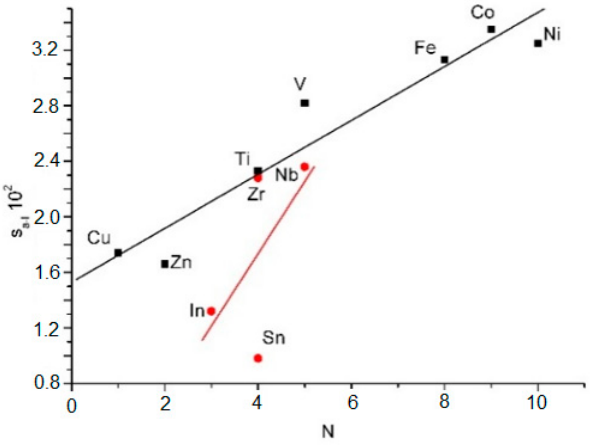

Figure 3. Dimensionless mass of autolocalizon as a function of the of electron number per unit cell: ■ for metals from 4th period; • for metals from 5th period of the Periodic Table of Elements.

3.1.3. Nature of the Effective Mass

Let us consider instead of masses $m_{ef}^{(emp)}$ found from Equation (1), masses $m_{ef}^{(cal)} = \rho r_{ion}^3$ close in values but calculated independently from reference data. Here, ρ is the density of the material, r_{ion} is the ionic radius, and r_{ion}^3 is the volume per ion in the crystal lattice of a metal. In that case, Equation (1) assumes the form

$$\lambda V_{aw} m_{ef}^{(cal)} = (\lambda V_{aw}) \cdot (\rho r_{ion}^3) = \varsigma, \quad (6)$$

relating the characteristics of the autowave processes of the localized plastic flow λ and V_{aw}, found experimentally [29], and the material characteristics ρ and r_{ion} of the deformable medium, determined independently by other researchers.

Results of calculations of the parameter ς of Equation (6) for the investigated metals are given in Table 2. The average parameter $\langle\varsigma\rangle = \sum_{i=1}^{19} \varsigma_i/19 = (6.9 \pm 0.45) \times 10^{-34}$ J·s appears unexpectedly close to the known Planck constant $h = 6.63 \times 10^{-34}$ J·s [30]; moreover, the ratio $\langle\varsigma\rangle/h = 1.04 \pm 0.06 \approx 1$.

Table 2. The values ς, calculated by Equation (6).

Parameter	**Metals**										
$\varsigma \cdot 10^{34}$	Cu	Zn	Al	Zr	Ti	V	Nb	α-Fe	ϒ-Fe	Ni	Co
	11.9	9.3	2.8	6.1	4.9	3.5	4.9	4.6	4.6	6.1	7.1
$\varsigma \cdot 10^{34}$	Sn	Mg	Cd	In	Pb	Ta	Mo	Hf	-	-	-
	8.9	4.9	7.4	9.9	18.4	5.5	3.0	7.3	-	-	-

The result according to which $\langle\varsigma\rangle$ and h are close to each other needs statistical testing. The standard statistical procedure used for this purpose consists in calculation of the Student's t-criterion [31]

$$\hat{t} = \frac{\langle\varsigma\rangle - h}{\sqrt{\hat{o}^2}} \cdot \sqrt{\frac{n_1 \cdot n_2}{n_1 + n_2}} \tag{7}$$

and its subsequent comparison with the chosen standard criterion $\hat{t}_{0.05} =$ for a 0.95 confidence level. In Equation (7), $n_1 = 19$ is the number of ς_i values obtained from Equation (6), and $n_2 = 1$. The last condition means that the Planck constant was determined with high accuracy—that is, with zero variance [30]. Under such circumstances, the estimated total variance of $\langle\varsigma\rangle$ and h is calculated as

$$\hat{o}^2 = \frac{\sum\limits_{i=1}^{n_1}(\varsigma_i - \langle\varsigma\rangle)^2 + \sum\limits_{1}^{1}(h-h)^2}{n_1 + n_2 - 2} = \frac{\sum\limits_{i=1}^{n_1}(\xi_i - \langle\varsigma\rangle)^2}{n_1 + n_2 - 2}. \tag{8}$$

From Equations (7) and (8), it follows that $\hat{t} = 0.046 << \hat{t}_{0.05} = 2.13$, where $\hat{t}_{0.05}$ is the value of the Student's criterion for a 0.95 confidence level, and the number of degrees of freedom is $n_1 + n_2 - 2 = 18$. Hence, the difference between $\langle\varsigma\rangle$ and the Planck constant h is statistically insignificant, and the corresponding samples belong to one general population. Thus, $\langle\varsigma\rangle$ calculated from Equation (6) is the Planck constant, and the plastic deformation phenomenon acquires formal relationship with the quantum-mechanical phenomena. The possibility itself of determining the Planck constant from rather rough measurements of the length and velocity of the localized strain-induced autowave seems surprising. However, this fact suggests that quantum-mechanical laws play a more important role in plasticity physics than it is customary to consider.

Nowadays, it is natural to postulate the existence of the quasi-particle associated with the autowave process [5] considering that the effective mass defined by Equation (1) is indeed its mass. This quasi-particle is called autolocalizon [32,33]. Here, it must be taken into account that the developing reasons can be applied only to the phase autowave of the localized plastic flow for which it is possible to measure sufficiently reliably the parameters λ and V_{aw} [29]. The autolocalization characteristics, estimated from their relationships with the localized plastic flow autowaves, are given in Table 3.

Table 3. The principal characteristics of autolocalizon.

Characteristic	**Formula**	**Value**
Dispersion law	$\omega(k) \sim 1 + k^2$	-
Mass (amu)	$m_{a-l} \equiv m_{ef} = h/\lambda V_{aw}$	1.7 ± 0.2
Velocity (m/s)	$V_{a-l} \equiv V_{aw}$	10–5 … 10–4
Momentum (J·s/m)	$p = \hbar k = h/\lambda$	(6 … 7)·10–32

3.2. Autolocalizon and Localized Plastic Flow

Now it is necessary to demonstrate that the introduction of the autolocalizon simplifies the explanation of the special features of plastic flow kinetics, in particular, associated with stress or strain jumps. Here, we use the quasi-particle approach to reach some of these goals.

3.2.1. Some Characteristics of Autowave Plastic Flow

First, it is necessary to discuss some details of the Portevin–Le Chatelier effect manifested through jump-like stress increments and decays of the deforming stress caused by them. This effect is often observed during deformation of binary Al-Cu or Al-Mg alloys and has been studied in ample detail [6,28,34–38]. During jump-like deformation, the sample lengthens discretely, and the amplitude of each jump is determined by the properties of the deforming material.

Analyzing this phenomenon, we use the natural assumption that an integer number $m = 1, 2, 3, \ldots$ of autowaves with length λ fits into the sample length. In this case (see Figure 4), Equation (1) is written in the form

$$\lambda = \frac{h}{\rho r_{ion}^3 V_{aw}} \tag{9}$$

so that with strain growth, the sample length increases by

$$\delta L \approx \lambda m \approx \frac{h}{\rho r_i^3 V_{aw}} \cdot m \sim m. \tag{10}$$

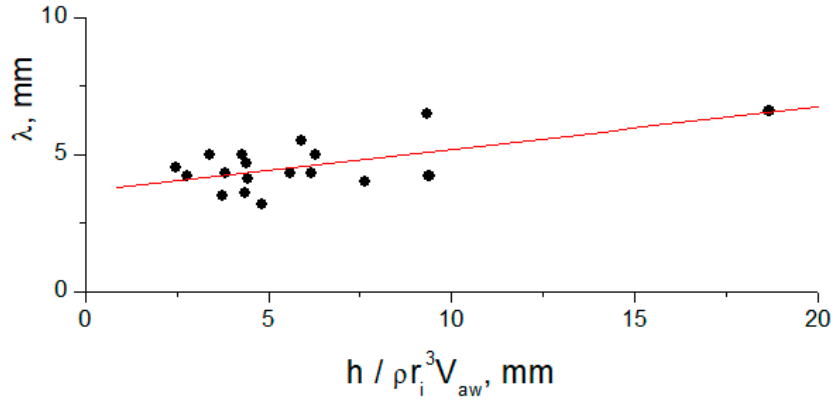

Figure 4. Verification of Equation (9). Values of the wavelengths λ and velocities V_{aw} were evaluated from the $X - t$ diagrams (see Figure 2), and values of ion radius r_i and density ρ were borrowed from the handbooks.

Equation (10) can be used to estimate the jump-like sample elongation δL if m = 1, $V_{aw} \approx 3 \times 10^{-3}$ m/s, and $\rho \cdot r_i^3 \approx 1.7$ amu $\approx 3 \times 10^{-27}$ kg. Under these conditions, $\delta L \approx 10^{-4}$ m. This is in agreement with the experimentally observed jump length caused by the Portevin–Le Chatelier effect [28].

It follows from Equation (10) that the sample length changes discretely. This means that the jump-like deformation can be considered as a process of fine tuning of the sample length to the existing autowave pattern of plastic strain localization, and Equation (10) becomes obligatory in character. In addition, from Equation (10) it follows that $\delta L \sim V_{aw}^{-1}$. The data presented by us in [29] demonstrate that the autowave velocity is proportional to the velocity of the traverse of a test machine—that is, $V_{aw} \sim V_{mach}$ In this case, a decrease in the jump amplitude should be expected with increasing stretching rate. There are convincing experimental evidences of such change—for example, in [39] for deformation of aluminum at the temperature of 1.4 K.

3.2.2. Autowave Length as the Free Path Length of the Autolocalizon

It is well-known that all the quasi-particles are unobservable in principle. Their existence can be verified by the calculations of the quantities founded experimentally. The example of similar evaluation is considered below for the length of localized plastic flow autowave.

In the context of the quasi-particle approach, a deforming medium can be considered as a binary mixture of quasi-particles of two kinds: phonons and autolocalizons. In this case, quantitative laws of plastic flow can be explained by the Brownian motion of autolocalizons in the viscous phonon gas. Such characteristic, as the autowave length $\lambda \approx 10^{-2}$ m, important for autowave processes of plastic flow localization, can be identified with the length of the resultant displacement $R = \left(\sum_{i=1}^{i=n} r_i^2\right)^{1/2}$ [40] in the process of the Brownian random walk of autolocalizons in the phonon gas during the time $\tau = 2\pi/\omega \approx 10^3$ s. Thus, according to [40],

$$R \approx \sqrt{\frac{k_B T}{\pi B r_{a-l}} \cdot \tau} \approx \sqrt{\frac{2k_B T}{\omega B r_i}} \tag{11}$$

where k_B is the Boltzmann constant. If we accept that the autolocalizon radius is $r_{a-l} \approx r_{ion} \approx 10^{-10}$ m and that the dynamic viscosity of phonon gas is $B \approx 10^{-4}$ Pa·s [23], then the displacement at T = 300 K will be $R \approx 10^{-2}$ m—that is, it will agree with the length λ of the localized deformation autowave.

3.2.3. Elastic-Plastic Invariant of Deformation and Autolocalizon

From Equation (11) it follows that the quantity

$$\frac{R^2\omega}{2\pi} \approx \frac{k_B T}{\pi B r_{a-l}} \approx 1.3 \cdot 10^{-7} m^2/s \tag{12}$$

can be identified with the product λV_{aw} with which it coincides by dimensionality and value [29]. In that case, the basic equation of autowave mechanics of plasticity—the elastic-plastic invariant of deformation (see Figure 5)—can be re-written as

$$\hat{Z}_{calc} \equiv \frac{\lambda V_{aw}}{\chi V_t} = \frac{k_B T}{\pi B r_{ion} \chi V_t} \approx \frac{h\omega_D}{\pi B r_{ion} \chi V_t}. \tag{13}$$

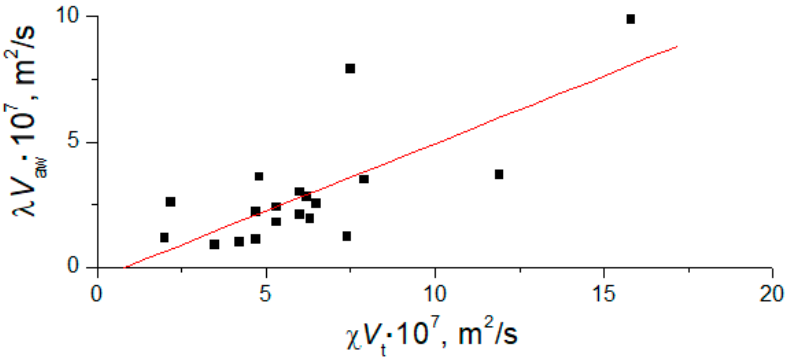

Figure 5. Verification of the elastic-plastic invariant of deformation (13).

Here, χ is the interplanar distance and V_t is the transverse ultrasonic wave rate in a crystal [1]. Equation (13) is valid by $T > T_D$, when all thermal vibrations have been excited in the crystal, and it is possible to set $k_B T_D \approx \hbar\omega_D$.

Evidently, the value $\hat{Z}_{calc}$ calculated with the help of Equation (13) is defined only by the material (lattice) constants. Results of its calculations are given in Table 4.

The average calculated value is $\langle \hat{Z} \rangle_{calc} = 0.48 \pm 0.1$, and the ratio $\langle \hat{Z} \rangle_{exp} / \langle \hat{Z} \rangle_{calc} = 0.97 \approx 1$—that is, it almost coincides with the experimentally observed value.

This conclusion is important, because it demonstrates that the elastic-plastic strain invariant is a versatile characteristic of the deforming medium. Equation (13) can be used to calculate this parameter,

knowing in fact only one characteristic of the plastic deformation process, namely, the phonon gas viscosity B. Thus, by introduction of the autolocalizon, some problems of solid state plasticity have been solved. This proves the correctness of the idea being developed.

Table 4. Calculated and experimentally founded values $\hat{Z}$.

Value	**Metals**										
	Cu	Zn	Al	Zr	Ti	V	Nb	α-Fe	ϒ-Fe	Ni	Co
$\hat{Z}_{calc}$	0.75	0.31	1.05	0.55	0.32	0.45	0.33	0.54	0.34	0.35	0.5
$\hat{Z}_{exp}$	0.42	0.5	4.47	0.33	0.42	0.85	0.44	0.46	0.48	0.35	0.38
	Sn	Mg	Cd	In	Pb	Ta	Mo	Hf			
$\hat{Z}_{calc}$	0.65	0.63	0.27	1.18	1.4	2.7	0.4	0.33			
$\hat{Z}_{exp}$	0.48	0.98	0.24	0.78	0.5	1.1	0.2	0.24			

4. Discussion

4.1. Elementary Excitation Spectrum of a Plastically Deforming Medium

In general, the deformation processes involve interrelated elastic waves and plastic autowaves whose interaction provides the basis for the construction of the two-component localized plastic flow model proposed in [29]. The well-known dispersion relations characterize both components. The close relationship between the elastic and plastic deformation components allows us to potentially obtain a common dispersion law for the elastic and plastic strains.

4.1.1. Hybridized Spectrum of an Elastic-Plastic Medium

The model relating the acoustic and deformation processes in solids envisages the possibility of hybridization of the elementary excitation spectra of the elastic (phonon) and deformation (autolocalizon) subsystems. The hybridized spectrum can be obtained by overlaying the linear dispersion relation for transverse phonons $\omega \approx V_t k$ far away from the Brillouin zone boundary—i.e., at $\omega \to \omega_D$ [25]—and the parabolic curve of the dispersion relation for localized plasticity autowaves (autolocalizons) [29]. The result of such overlay for polycrystalline aluminum is shown in Figure 6.

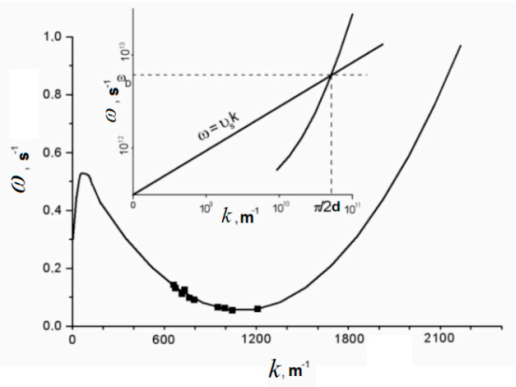

Figure 6. Generalized dispersion law for localized plastic flow autowaves ($\omega \sim 1 + k^2$) and elastic waves ($\omega \sim k$); in the insert, the high-frequency range of spectrum is represented.

The estimate shows that the coordinates of the intersection point of the plots for high-frequency range are physically justified: $\hat{\omega} \approx \omega_D \approx 10^{13}$ Hz, and the wave number $\hat{k} = 2\pi/\hat{\lambda}$ corresponds to the minimal possible wavelength $\lambda_{\min} = \hat{\lambda} \approx 2\chi$. This confirms the applicability of the plastic flow description by the interaction of the phonon gas and the quasi-particles (autolocalizons).

The situation near the point of intersection of the linear and parabolic dependences in the low-frequency region is more interesting at small values of the wave number where the hybridized

dependence $\omega(k)$ has a local maximum. Its existence can be due to dislocations induced by elastic nonlinear strain of initially defect-free crystal according to the mechanism of condensation of long-wavelength phonons proposed in [41]. Individual dislocations appearing because of this process are unstable, but their energy decreases with decreasing or increasing wave number k. We can assume that the first case corresponds to the formation and development of the low-energy dislocation structures [42] (in the limit of the localized plastic strain autowaves), and the second case leads to the origin of fragile microcracks because of interaction of a small number of dislocations.

According to the dispersion relation for autowaves of localized plastic flow, in the vibrational spectrum $\omega(k)$ there is a gap at $0 \leq \omega_0 \approx 10^{-2}$ Hz. Since at any temperature $\hbar\omega_0 << k_B T$, the spontaneous plastic strain localization should be excited at temperatures as low as is wished. Indeed, the jump-like deformation associated with flow localization was repeatedly observed at $T \leq 1$ K [39]. The hybridized dependence $\omega(k)$ shown in Figure 6 demonstrates its striking similarity to the dispersion curve $E(k)$ of superfluid helium [5]. The minimum in the parabolic branch of this curve corresponds to the creation of rotons–elementary excitations in the medium with a quadratic dispersion law. This suggests that the autolocalizon is an analog of the roton created by the localized plastic strain and determines the kinetics of this process.

4.1.2. Autolocalizon Dispersion and Effective Mass

Using the dispersion relation for the localized plasticity autowaves [1,29], it is possible to calculate by the standard method [5] the effective autolocalizon mass corresponding to the localized plastic flow of the autowave:

$$m_{a-l} = \hbar \frac{\partial^2}{\partial k^2}[\omega(k)], \tag{14}$$

equal to 0.1 amu for Al and 0.6 amu for Fe. The effective masses calculated from Equation (1) $m_{ef} = h/\lambda V_{aw}$ and given in Table 1 are 0.5 and 1.8 amu for aluminum and iron, respectively—that is, they have the same orders of magnitude. These estimates confirm the correctness of the assumption that quasi-particles (autolocalizons) with an average mass of ~1.7 amu are associated with the aotowave processes of plastic flow localization. According to [5], the effective roton mass is m_{rot} =0.64 amu. The close values of the effective masses of the autolocalizon and the roton also testify in favor of the above-discussed hypothesis.

4.1.3. Condensation of Quasi-Particles during Plastic Flow

There is interesting possibility to refine the nature of the elastic-plastic strain invariant. Equation (13) for the elastic-plastic invariant written in the form (see Figure 7)

$$\frac{h}{\lambda V_{aw}} = 2\frac{h}{\chi V_t} \tag{15}$$

makes sense of the equality of masses, where $h/\lambda V_{aw} = m_{a-l}$ is the de Broglie autolocalization mass and $h/\chi V_t = m_{ph}$ is the phonon mass.

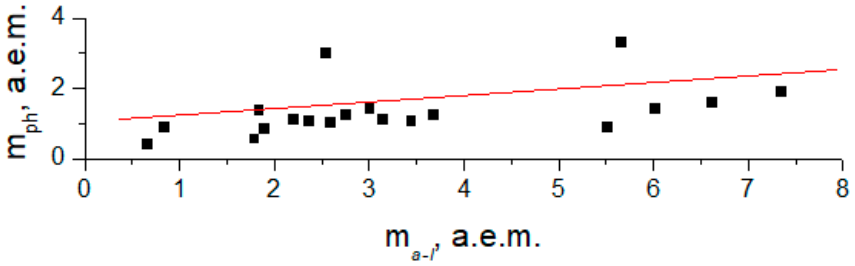

Figure 7. Correlation dependence of phonon and autolocalizon masses for Equation (15).

In this case, Equation (15) is reduced to the equality $m_{a-l} \approx 2m_{ph}$ that can be considered as the condition of creation of the autolocalizon with the momentum

$$p_{a-l} = (m_{a-l}V_{aw}) = \left[2\left(m_{ph}V_t\right)^2(1+\cos\alpha)\right]^{1/2} = \sqrt{2}m_{ph}V_t(1+\cos\alpha)^{1/2}, \quad (16)$$

as shown in Figure 8. Here, 2 is the angle between the momenta of phonons.

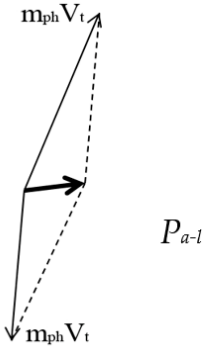

Figure 8. A scheme of autolocalizon generation in a two-phonon process. P_{a-l} is a momentum of autolocalization.

The probability of this process was first calculated in [43] to explain the creation of rotons in superfluid helium. Reissland [44] considered the process of combining two phonons into one in detail. The process discussed in the present work is close to the quantum mechanism of defect formation in crystals considered in [41]. It was demonstrated in this work that the creation of dislocations and dislocation ensembles (dislocation walls, grain boundaries, and other defects) in an ideal crystal is the result of Bose's condensation of long-wavelength phonons under the influence of deformation or temperature.

The foregoing provides the basis for the development of new representations on the stages of the localized plastic flow of solids. According to these representations, quasi-particles of definite types correspond to each deformation stage. The collapse of the localized plastic flow autowave observed at the stage of prefailure of materials described in [29] is a typical example of this condensation of quasi-particles in a plastic flow. This process can be considered as the production of the crackon [13]—that is, as the beginning of the failure process.

Experimental data allow us to describe qualitatively the process of generation of structural defects. At the stage of elastic deformation, only phonons, which redistribute the elastic stresses over the crystal, exist in the crystal. In the process of phonon condensation, according to the mechanism proposed by us in [41], the plastic shear quanta (dislocations) are formed in the crystal, thereby giving rise to the plastic flow. The intermediate stages at which the defects of the above-mentioned types, such as dilatons, frustrons, or the so-called dislocation precursors [45–47], can precede the stage of dislocation formation. Finally, the collapse of the localized plastic flow autowaves can be considered as the process of condensation of the autolocalizons with formation of the destruction quantum–crackon and its further motion during cracking.

4.1.4. General Meaning of Autolocalizon Introduction

The amazingly close values of the parameter $\langle\varsigma\rangle$ calculated from Equation (6) considered above, which contains the macroscopic parameters λ and V_{aw} that are determined experimentally, to the reference value of the Planck constant h indicate a direct relationship of the macroscopic localization phenomena of plastic flow with the properties of the lattice. With application to the process of localized plastic flow, this means that the spatiotemporal microstructural inhomogeneity of the deforming medium (the dislocation submicrostructure) defines much less the measurable macromechanical

characteristics, such as the flow stress, yield point, work hardening coefficient, and plastic flow localization pattern than it is supposed in traditional dislocation models.

For these reasons, we can determine that the mechanical properties are substantially controlled by the lattice characteristics of the elastic medium and hence, by the laws of quantum mechanics. From this point of view, the obvious importance of Equation (6) relating the quantities that are traditionally considered as diverse is additionally confirmed. The existence of such relationship has been conventionally neglected in different plastic flow models; however, Equation (6) explicitly indicates wrongfulness of this opinion.

4.1.5. Plastic Flow as a Macroscopic Quantum Phenomenon

The consistent development of representations stated above suggests the opportunity to refer the localized plastic flow to a series of macroscopic quantum phenomena, such as superfluidity, superconductivity [48], and quantum Hall's effect [49]. The quantization of the corresponding characteristics of the medium in these phenomena is manifested on the macroscopic scale and can be observed directly (Table 5); the macroscopic equations describing these characteristics involve the Planck constant.

Table 5. Macroscopic quantum phenomena.

Phenomenon	**Quantum Characteristic**	
	Value	**Formula**
Superconductivity [5]	Magnetic flux	$\Phi = \frac{\pi\hbar c}{e} \cdot m$
Superfluidity [5]	Rotational velocity of vortices in superfluidity HeII	$v = \frac{\hbar}{A_{He}} \cdot \frac{1}{r} \cdot m$
Quantum Hall effect [49]	The Hall resistance	$R_H = \frac{h}{e^2} \cdot \frac{1}{m}$
Serrated plastic deformation	Elongation during deformation jump	$\delta L = \frac{h}{\rho r_{ion}^3 V_{aw}} \cdot m$

Notation: e is the electron charge, c is the speed of light, r is the radius of the vortex, m = 1, 2, 3 . . . .

Formally, the possible quantum character of the plastic flow is indicated by the close analogy between the forms of dispersion curves for the plastic flow autowaves and for superfluid helium [5] shown in Figure 6. Moreover, it can be noted that the quadratic dispersion curve of the localized plasticity autowaves is similar to the spectrum of elementary excitations in a superconductor [5].

The similarity of physical natures of the macroscopic phenomena is because the effects underlying them do not admit a description in the context of models based largely on the additive properties of individual strain carriers. For the plastic flow, the dislocations, each of which describes "the shear quantum", can be considered as such carriers [50].

There are some additional reasons in favor of the above-considered formal similarity between the plastic flow and the superfluidity. Indenbom [51] first paid attention to the analogy between the dislocations and quantum vortices in superfluid helium or quantized flows in the second-order superconductors. This analogy can be expanded if we consider that in a deforming material, as well as in superfluid helium, two regimes of motion co-exist with different velocities. First, this is slow motion of separate volumes accompanying the change of the body shape as a whole, and second, this is motion of dislocations with high velocities providing this change of the body shape. The high viscosity of the crystal material $\eta \approx 10^6$ Pa·s [6] corresponds to the first of them, whereas the low viscosity of the phonon gas $B \approx 10^{-4}$ Pa·s [23] corresponds to the second of them. It is well known that the velocity of viscous motion is proportional to the applied force and inversely proportional to the viscosity [23]. Hence we can write down that $V = F_1/B$ or $V = F_1/\eta$, where $F_1 = \sigma L$ is the Peach-Kehler force per unit length of a dislocation [52]. For the phase autowave at the stage of linear work hardening, $\sigma >> 100$ MPa, $L \approx \lambda \approx 10^{-2}$ m, and $\eta \approx 10^6$ Pa·s. The estimated velocity is in agreement with $V_{aw} \approx$

10^{-5} m/s observed in [28]. At low viscosity $B \approx 10^{-4}$ Pa·s, we obtain $V_{disl} \approx 10^{2}$ m/s, which is in agreement with the velocity of dislocation motion over the barrier [23].

A similar approach based on the quantum-mechanical representations seems surprising for experts in plasticity physics, since the spatial scale of the macroscopic plasticity phenomena considerably exceeds the scales for which the quantum approach is traditionally used. Thus, the ratio of the autowave ($\lambda \approx 10^{-2}$ m) and dislocation ($b \approx 10^{-10}$ m) scales $\lambda/b \approx 10^{8}$. However, already on the dislocation level, the strain quantization seems natural, at least because of the stepwise behavior of the crystal lattice, and the Burgers vector b can be interpreted as a shear strain quantum, as pointed out by many authors [24,41,50]. Thus, the use of the wave-quasi-particle dualism for a description of strain localization processes is quite justified.

5. Conclusions

The close relationship of the plasticity effects with the crystal lattice characteristics during macroscopic plastic deformation is a possible reason for the existence of quantum effects in the macroscopic strain processes. In other words, generation of the localized plastic flow autowaves—self-organization of the deforming medium—is realized in the elastic medium whose behavior is governed by laws of the quantum mechanics. Therefore, the energy redistribution in the process of forming the localized plasticity autowaves in the system capable of self-organization is also subordinate to the quantum nature of crystals.

Experimental results and their interpretation indicate the importance of the consideration of the close interrelation of defect ensembles with the phonon subsystem in crystals. Such interrelation can be described correctly both by the mechanism of interaction of waves and autowaves and by the mechanism of interaction of quasi-particles, phonons and autolocalizons. The two-component model of the plastic flow developed on this basis correctly explains the correlations of the macroscopic scale during plastic flow localization in deforming metals and alloys. Thus, the quasi-particle approach completes the traditional analysis of plastic flow phenomenon. This suggests that auto-localizon can be used for the development of the physical theory of plasticity.

Author Contributions: Both authors contributed to the manuscript. Conceptualization, L.B.Z.; Investigation, S.A.B. The manuscript was prepared by L.B.Z. and S.A.B. All authors have read and agreed to the published version of the manuscript.

Funding: The research was founded by Russian Scientific Foundation, grant No. 16-19-10025 P.

Acknowledgments: We thank our colleagues in the Strength Physics Laboratory of ISPMS SB RAS for helpful discussion of this study.

Conflicts of Interest: The authors declare no conflict of interest.

References

1. Zuev, L.B.; Barannikova, S.A. Autowave physics of material plasticity. *Crystals* **2019**, *9*, 458. [CrossRef]
2. Zuev, L.B. Autowave mechanics of plastic flow in solids. *Phys. Wave Phenom.* **2012**, *20*, 166–173. [CrossRef]
3. Zuev, L.B. Wave phenomena in low-rate plastic flow of solids. *Ann. Phys.* **2001**, *10*, 965–984. [CrossRef]
4. Zuev, L.B. On the waves of plastic flow localization in pure metals and alloys. *Ann. Phys.* **2007**, *16*, 287–310. [CrossRef]
5. Brandt, N.B.; Kulbachinskii, V.A. *Quasi-Particles in Condensed State Physics*; Fizmatlit: Moscow, Russia, 2007; 631p.
6. Bell, J.F. *Mechanics of Solids*; Springer: Berlin/Heidelberg, Germany, 1973; 596p.
7. Steverding, B. Quantization of stress waves and fracture. *Mater. Sci. Eng.* **1972**, *9*, 185–189. [CrossRef]
8. Maugin, G.A. Solitons in elastic solid. *Mech. Res. Commun.* **2011**, *38*, 341–349. [CrossRef]
9. Gilman, J.J. Escape of dislocations from bound states by tunneling. *J. Appl. Phys.* **1968**, *39*, 6086–6090. [CrossRef]
10. Oku, T.; Galligan, J.M. Quantum mechanical tunneling of dislocations. *Phys. Rev. Lett.* **1969**, *22*, 596–597. [CrossRef]

11. Petukhov, B.V.; Pokrovskii, V.L. Quantum and classic motion of dislocations in the potential Peierls relief. *J. Exp. Theor. Phys.* **1972**, *63*, 634–647.
12. Iqbal, S.; Sarwar, F.; Rasa, S.V. Quantum mechanics tunneling of dislocations: Quantization and depinning from Peierls barrier. *World J. Cond. Mater. Phys.* **2016**, *6*, 103–108.
13. Morozov, E.M.; Polak, L.S.; Fridman, Y.B. On variation principles of crack development in solids. *Sov. Phys. Dokl.* **1964**, *156*, 537–540.
14. Zhurkov, S.N. Dilaton mechanism of the strength of solids. *Solid Stat. Phys.* **1983**, *25*, 1797–1800.
15. Olemskoi, A.I.; Katsnelson, A.A. *A Synergetic of Condensed Medium*; URSS: Moscow, Russia, 2003; 335p.
16. Billingsley, J.P. The possible influence of the de Broglie momentum-wavelength relation on plastic strain "autowave" phenomena in "active materials". *Int. J. Solids Struct.* **2001**, *38*, 4221–4234. [CrossRef]
17. Danilov, V.I.; Barannikova, S.A.; Zuev, L.B. Localized Strain Autowaves at the Initial Stage of Plastic Flow in Single Crystals. *Tech. Phys.* **2003**, *48*, 1429–1435. [CrossRef]
18. Zuev, L.B.; Danilov, V.I. Plastic deformation viewed as evolution of an active medium. *Int. J. Solids Struct.* **1997**, *34*, 3795–3805. [CrossRef]
19. Zuev, L.B.; Danilov, V.I. A self-excited wave model of plastic deformation in solids. *Philos. Mag. A* **1999**, *79*, 43–57. [CrossRef]
20. Zuev, L.B. The linear work hardening stage and de Broglie equation for autowaves of localized plasticity. *Int. J. Solids Struct.* **2005**, *42*, 943–949. [CrossRef]
21. Zuev, L.B.; Danilov, V.I.; Barannikova, S.A.; Zykov, I.Y. Plastic flow localization as a new kind of wave processes in solids. *Mater. Sci. Eng. A* **2001**, *319–321*, 160–163. [CrossRef]
22. Landau, L.D.; Lifshits, E.M. *Course of Theoretical Physics. Fluid Mechanics*; Pergamon Press: Oxford, UK, 1987; Volume 6, 539p.
23. Alshits, V.I.; Indenbom, V.L. Mechanisms of dislocation drag. In *Dislocations in Crystals*; Nabarro, F.R.N., Ed.; North-Holland: Amsterdam, The Netherlands, 1986; Volume 7, pp. 43–111.
24. Eshelby, J.D. Continual theory of defects. *Solid Stat. Phys.* **1956**, *3*, 79–173.
25. Newnham, R.E. *Properties of Materials*; University Press: Oxford, UK, 2005; p. 378.
26. Bobrov, V.S.; Zaitsev, S.I.; Lebyodkin, M.A. Statistics of dynamic processes at low temperature serrated deformation of metals. *Phys. Solid Stat.* **1990**, *32*, 3060–3065.
27. Bobrov, V.S.; Lebyodkin, M.A. The role of dynamic processes at low temperature serrated deformation of aluminium. *Phys. Solid Stat.* **1993**, *35*, 1881–1889.
28. Lebyodkin, M.; Bougherira, Y.; Lebedkina, T.; Entemeyer, D. Scaling in the local strain-rate field during jerky flow in an Al-3%Mg alloy. *Metals* **2020**, *10*, 134. [CrossRef]
29. Zuev, L.B. Autowave Plasticity. In *Localization and Collective Modes*; Fizmatlit: Moscow, Russia, 2018; 208p.
30. Atkins, P.W. *Quanta. A Handbook of Conceptions*; Clarendon Press: Oxford, UK, 1974; 319p.
31. Hudson, D.J. *Statistics*; CERN: Geneva, Switzerland, 1964; 242p.
32. Zuev, L.B.; Barannikova, S.A.; Maslova, O.A. The features of localized plasticity autowaves in solids. *Mater. Res.* **2019**, *22*. [CrossRef]
33. Barannikova, S.A.; Danilov, V.I.; Zuev, L.B. Plastic strain localization in Fe-3%Si single crystals and polycrystals under tension. *Tech. Phys.* **2004**, *49*, 1296–1300. [CrossRef]
34. Lebyodkin, M.A.; Zhemchuzhnikova, D.A.; Lebedkina, T.A.; Aifantis, E.C. Kinematics of formation and cessation of type B deformation bands during the Portevin-Le Chatelier effect in an Al-Mg alloy. *Results Phys.* **2019**, *12*, 867–869. [CrossRef]
35. Kubin, L.P.; Chihab, K.; Estrin, Y.Z. The rate dependence of the Portevin—Le Chatelier effect. *Acta Metall.* **1988**, *36*, 2707–2718. [CrossRef]
36. Kubin, L.P.; Estrin, Y.Z. The critical condition for jerky flow. *Phys. Stat. Solid* **1992**, *172*, 173–185. [CrossRef]
37. Rizzi, E.; Hähner, P. On the Portevin—Le Chtelier effect: Theoretical modeling and numerical results. *Int. J. Plast.* **2004**, *29*, 121–165. [CrossRef]
38. Zaiser, M.; Aifantis, E.C. Randomness and slip avalanches in gradient plasticity. *Int. J. Plast.* **2006**, *22*, 1432–1455. [CrossRef]
39. Pustovalov, V.V. Serrated deformation of metals and alloys at low temperatures. *Phys. Low Temp.* **2008**, *34*, 871–913. [CrossRef]
40. Rumer, Y.B.; Ryvkin, M.S. *Thermodynamics, Statistical Physics and Kinetics*; Mir Publ.: Moscow, Russia, 1980; 600p.

41. Umezava, H.; Matsumoto, H. *Thermo Field Dynamics and Condensed States*; North-Holland Publ. Comp.: Amsterdam, The Netherlands, 1982; 504p.
42. Kuhlmann-Wilsdorf, D. The low energetic structures theory of solid plasticity. In *Dislocations in Solids, Nabarro, F.R.N., Duesbery, M.S., Eds.*; Elsevier: Amsterdam, The Netherlands, 2002; pp. 213–338.
43. Landau, L.D.; Khalatnikov, I.M. The theory of viscosity HeII. *J. Exp. Theor. Phys.* **1949**, *19*, 637–650.
44. Reissland, J.A. *The Physics of Phonons*; John Wiley and Sons LTL: London, UK, 1973; 365p.
45. Psakhie, S.G.; Zolnikov, K.P.; Kryzhevich, D.S. Elementary atomistic mechanism of crystal plasticity. *Phys. Lett. A* **2007**, *367*, 250–253. [CrossRef]
46. Psakhie, S.G.; Shilko, E.V.; Popov, M.V.; Popov, V.L. The key role of elastic vortices in the initiation of shear cracks. *Phys. Rev. E* **2015**, *91*, 63302.
47. Dmitriev, A.I.; Nikonov, A.Y.; Filippov, A.E.; Psakhie, S.G. Molecular Dynamics Study of the Evolution of Rotational Atomic Displacements in a Crystal Subjected to Shear Deformation. *Phys. Mesomech.* **2019**, *22*, 375–381. [CrossRef]
48. Tilley, D.R.; Tilley, J. *Superfluidity and Superconductivity*; IOP Publ.: Bristol, UK, 1990; 268p.
49. Imry, Y. *Introduction to Mesoscopic Physics*; University Press: Oxford, UK, 2002; 236p.
50. Katanaev, M.O. Geometric theory of defects. *Phys. Uspekhi* **2005**, *175*, 705–733. [CrossRef]
51. Indenbom, V.L. The structure of real crystals. In *The Modern Crystallography*; Vainstein, B.K., Fridkin, V.M., Indenbom, V.L., Eds.; Nauka Publ.: Moscow, Russia, 1979; pp. 297–341.
52. Hull, D.; Bacon, D.J. *Introduction in Dislocations*; Elsevier: Oxford, UK, 2011; 272p.

Publisher's Note: MDPI stays neutral with regard to jurisdictional claims in published maps and institutional affiliations.

© 2020 by the authors. Licensee MDPI, Basel, Switzerland. This article is an open access article distributed under the terms and conditions of the Creative Commons Attribution (CC BY) license (http://creativecommons.org/licenses/by/4.0/).